

# Recent Advances in Large-Scale Structure and Galaxy Formation Studies

L. Guzzo<sup>a\*</sup>

<sup>a</sup>INAF - Osservatorio Astronomico di Brera  
Via Bianchi 46, I-23807 Merate (LC), Italy

I review recent progress in the study of the large-scale structure of the Universe, covering the following areas: (1) Results from recently completed or ongoing redshift surveys of galaxies and X-ray clusters; (2) Measurements of the power spectrum of fluctuations approaching Gpc scales; (3) Redshift-space distortions and their cosmological use; (4) Structure at high redshifts and its connection to galaxy formation.

## 1. INTRODUCTION

It is a particularly fortunate moment to review the field of large-scale structure<sup>2</sup>, in the light of the impressive series of results that appeared during the last year or so, as a consequence of the (entire or partial) completion of large surveys of galaxies and clusters of galaxies. The enthusiasm for the new large-scale structure measurements has been further animated by the immediate possibility to compare them to the recent fundamental results obtained by microwave background experiments, which measured with unprecedented precision the power spectrum of anisotropies over scales finally overlapping those probed by galaxy surveys (see De Bernardis, this volume). In this brief non-specialist review I have tried and assess this enthusiasm, in the spirit of providing a general, though clearly incomplete, guide to what seem to me the most promising recent results on large-scale structure in the local Universe. Some emphasis is placed on the importance of understanding the “bias”, i.e. the relation between the distribution of the objects under study and the matter whose gravity governs the overall evolution of clustering. Finally, prospects for studying such evolution through deep surveys of galaxies are quickly touched in the last section.

The recent flow of results makes it even more

difficult for such a brief review to be complete, or at least balanced. I therefore apologize to those colleagues whose work was inadvertently overlooked. The time scale is tuned to September 2001, but I have added a few references until January 2002 which seemed helpful for a clearer picture.

## 2. COSMOLOGICAL FRAMEWORK

Let us set the basic scene for interpreting the observations we shall discuss here. It will be interesting, at the end, to verify whether the assumed framework is corroborated by the latest results.

The current “standard” model for the origin and evolution of structure in the expanding Universe is the Cold Dark Matter (CDM) model [1], whose global features provide a framework which is remarkably consistent with a large number of observations. The “Cosmology 2000” version of the model, which takes into account the independent evidences for a flat geometry (from the angular power spectrum of anisotropies in the Cosmic Microwave Background [2]) and an accelerated expansion (from the luminosity-distance relation of distant supernovae, used as “standard candles” [3]) is one where CDM, in the form of some kind of weakly-interacting non-relativistic particles (see pertinent articles in this volume), contributes about 30% of the total density, with the remaining 70% provided by a “dark energy” associated to a *Cosmological Constant*. I will comment at the end of this review on how com-

\*e-mail: guzzo@merate.mi.astro.it

<sup>2</sup>Review to appear in *Topics in Astroparticle and Underground Physics - TAUP2001*, (LNGS, September 2001), Nucl.Phys. B, A. Bettini et al. eds., Elsevier



### 3. PROGRESS IN LARGE-SCALE STRUCTURE STUDIES

#### 3.1. Galaxy Redshift Surveys

Since the 1970's, redshift surveys of galaxies are the primary way to reconstruct the 3D topology of the Universe [15]. Last year has seen the completion and public release [16] of the first 100,000 galaxy redshift measurements by the Anglo-Australian 2dF Galaxy Redshift Survey<sup>4</sup>, the largest complete sample of galaxies with measured distances to date [16]. This survey includes all galaxies with blue magnitude  $b_J$  brighter than  $\sim 19.5$ , mainly over two areas covering  $\sim 2000$  square degrees in total, to an effective depth of about  $600 h^{-1} \text{Mpc}$  ( $z \sim 0.2$ ). The immediate precursors of this survey [17,18] reached a similar depth, but over much smaller areas: for comparison, the Las Campanas Redshift Survey (LCRS [17]), completed in 1996, measured a total of 16,000 redshifts, compared to the 250,000 that will eventually form the full 2dF survey. A plot of the galaxy distribution within the two main sky regions of this survey is shown in Fig.1. Here one can appreciate in detail the wealth of structures typical of the distribution of galaxies: clusters, superclusters (filamentary or perhaps sheet-like) and regions of very low density, the *voids* [15]. A number of important results have been published in 2001 and are continuing to appear from the first completed part of the survey. I will discuss some of them in more detail in the following sections (see also [21] for an overview).

In a parallel effort, the Sloan Digital Sky Survey (SDSS)<sup>5</sup> is on its way covering a large fraction of the Northern sky with a CCD survey in five photometric bands ( $u'$ ,  $g'$ ,  $r'$ ,  $i'$ ,  $z'$ ), while in parallel measuring redshifts for one million galaxies over the same area [22]. The SDSS photometric survey reaches a typical red magnitude  $r' \sim 23$ , with the galaxy redshift survey being limited to  $r' = 17.7$ . The SDSS has also released an early fraction of its data (<http://archive.stsci.edu/sdss/>), including photometry and spectroscopy over 462 square degrees. There is no doubt that this represents

the largest and most comprehensive galaxy survey work ever conceived. The multi-band photometric survey is going to be of immense value for a number of studies, as estimating *photometric redshifts* [23,24] to much larger depth than the direct spectroscopic survey, or select sub-samples of objects with well-defined colour/morphology properties. One relevant example of such colour selections has been the discovery of several high-redshift ( $z > 5$ ) quasars, including the  $z = 6.28$  case for which the first possible detection of the long-sought Gunn-Peterson effect, essentially the fingerprint of the “dark-ages”, has been recently reported [25]. Another important application will be the selection of about  $10^5$  “red luminous” galaxies with  $r' < 19.5$ , that will be observed spectroscopically providing a nearly volume-limited homogeneous sample of “old” galaxies out to a redshift  $z \simeq 0.5$ , by which to study the clustering power spectrum on extremely large scales and its evolution [26]. A detailed progress report on the SDSS has been presented at the meeting by Josh Freeman and the reader is addressed to the corresponding contribution for references to the first general analyses from the survey.

Both the 2dF and SDSS redshift surveys rely upon the large multiplexing performances of fiber-fed spectrographs, that allow the light from several hundred galaxies over a field of view of 1-2 degrees to be conveyed into the same slit on the spectrograph. This specific technology, in various forms, has been the key to the explosion of the redshift survey industry in the 1990's, bringing the efficiency from the 10 redshifts/night for galaxies brighter than blue magnitude  $b \sim 14$  of the 1970's, to the current 2500 redshifts/night to  $b \sim 19.5$  (see e.g. [27] for a more accurate account).

#### 3.2. Surveys of X-ray Clusters of Galaxies

Clusters of galaxies have a honourable history as a complementary tracer of large-scale structure (see e.g. [28]). Especially before the current era, when  $N > 100,000$  galaxy redshifts are becoming available over comparable volumes, groups and clusters have represented the most efficient alternative to map very large volumes of the Uni-

<sup>4</sup><http://www.mso.anu.edu.au/2dFGRS>

<sup>5</sup><http://www.sdss.org/>

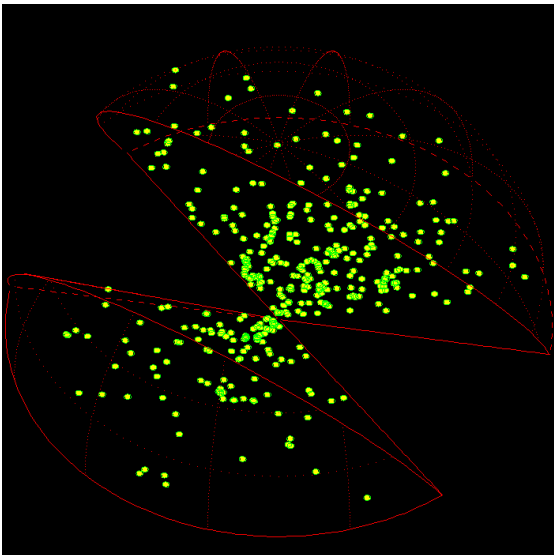


Figure 2. The spatial distribution of X-ray clusters in the REFLEX survey, out to  $600 h^{-1} \text{ Mpc}$  (from [13]). Note that here each point corresponds to a cluster, containing hundreds or thousands of galaxies. Structure is here mapped in a coarse way, yet sufficient to evidence very large structures as the “chains” of clusters visible in this picture.

verse, exploring in this way the gross structure and its statistical properties in the weak clustering regime.

X-ray selection represents currently the most physical way by which to identify and homogeneously select large numbers of clusters of galaxies<sup>6</sup> (see also discussion in [30]). Clusters shine in the X-ray sky thanks to the *bremsstrahlung* emission produced by a hot plasma ( $kT \sim 1 - 10 \text{ KeV}$ ) trapped within their potential wells. The bolometric emissivity (i.e., the energy released per unit time and volume) of this thin gas is proportional to its density squared and to  $T^{1/2}$ . Such dependence on  $n^2$  makes clusters stand out more

<sup>6</sup>A notable powerful alternative, so far limited by technical development, is represented by radio surveys using the Sunyaev-Zel’dovic effect. In this case one measures, in the radio domain, the CMB spectral distortions produced in the direction of a cluster by the Inverse Compton scattering of the CMB photons over the energetic electrons of the intracluster plasma (see e.g. [29] for a review).

in the X-rays than in the optical light (i.e. galaxy) distribution ( $\propto n$ ).

Under the assumption of hydrostatic equilibrium, the intracluster gas temperature, measured through the X-ray spectrum, is a direct probe of the cluster mass:  $kT \propto \mu m_p \sigma_v^2 \sim G \mu m_p M_{vir} / (3r)$  (where  $m_p$  is the proton mass,  $\mu \simeq 0.6$  the gas mean molecular weight,  $\sigma_v$  the galaxy 1D velocity dispersion and  $M_{vir}$  the cluster virial mass). X-ray luminosity, a more directly observable quantity with current instrumentation, shows a good correlation with temperature,  $L_X \propto T^\alpha$  with  $\alpha \simeq 3$  and a scatter  $\lesssim 30\%$ . The practical implication, even only on a phenomenological basis, is that clusters selected by X-ray luminosity are in practice mass-selected, with an error  $\lesssim 35\%$  (see e.g. [31] and references therein for a more critical discussion). Last, but not least, the selection function of an X-ray cluster survey can be determined to high accuracy, knowing the properties of the X-ray telescope used, in a similar way to what is usually done with magnitude-limited samples of galaxies [32]. This is of fundamental importance if one wants to compute statistical quantities and test cosmological predictions as, e.g., the mean density or the clustering of clusters above a given mass threshold [13].

Fig. 2 plots the large-scale distribution of X-ray clusters from the REFLEX (ROSAT-ESO Flux Limited X-ray) cluster survey, the largest redshift survey of X-ray clusters with homogeneous selection function to date [33]. This data set, completed in 2000 and publicly released at the beginning of 2002, is based on the X-ray all-sky survey performed by the ROSAT satellite in the early 1990’s (see e.g. [34,35] for a comprehensive summary). REFLEX includes 452 clusters over the southern celestial hemisphere and is more than 90% complete to a flux limit of  $3 \times 10^{-12} \text{ erg s}^{-1} \text{ cm}^{-2}$  (in the ROSAT energy band, 0.1-2.4 keV). The volume explored is larger than that of the 2dF survey and comparable to the volume that will be filled by the SDSS 1-million-galaxy redshift survey<sup>7</sup>. In the cluster distribu-

<sup>7</sup>The SDSS will then probe a much larger volume using a uniform sample of old (“Luminous Red”) galaxies selected through their colours out to  $z \sim 0.5$  [26].

tion the fine structure visible in Fig. 1 is obviously lost; however, a number of cluster agglomerates and filamentary structures with large sizes ( $\sim 100 h^{-1} \text{Mpc}$ ) are clearly evident, showing that clustering is still strong on such very large scales.

#### 4. STATISTICAL RESULTS ON LARGE-SCALE CLUSTERING

##### 4.1. The Power Spectrum of Fluctuations

We have seen that large-scale structure models as CDM are specified in terms of a specific shape for the power spectrum of density fluctuations  $P(k)$ . Analogously to standard signal theory, the power spectrum describes the squared modulus of the amplitudes  $\delta_k$  (at different spatial wavelengths  $\lambda = 2\pi/k$ ) of the Fourier components of the fluctuation field  $\delta = \delta\rho/\rho$  [4]. Studying the power spectrum of the distribution of luminous objects on sufficiently large scales, where the growth of clustering is still independent of  $k$ , we hope to recover a relatively undistorted information to test the models. The uncertainties in relating the observed  $P(k)$  of, e.g., galaxies to that from the theory are due to (a) nonlinear effects that modify the linear shape below some scale; (b) the relation between the luminous tracers for which we are measuring  $P(k)$  and the mass distribution, that is what the models predict. While the first problem can be circumvented by pushing redshift surveys to larger and larger scales (and/or following nonlinear evolution through numerical simulations), the second one involves knowing the so-called *bias* factor (or function). This can be defined as the ratio between the variances in galaxy counts and in the mass,  $(\delta n(r)/\langle n \rangle)_{rms} = b (\delta\rho(r)/\langle \rho \rangle)_{rms}$ . A significant amount of work has been dedicated to the problem of galaxy biasing during the last fifteen years, both theoretically (e.g. [36]) and observationally (e.g. establishing that for “normal” optically selected galaxies we have  $b \simeq 1 - 1.5$  over a fair range of scales [37]). However, understanding the physical origin of the bias involves comprehending the details of how the (mainly dark matter) mass of a galaxy governs the visible stellar light we use to select it for our surveys. De-

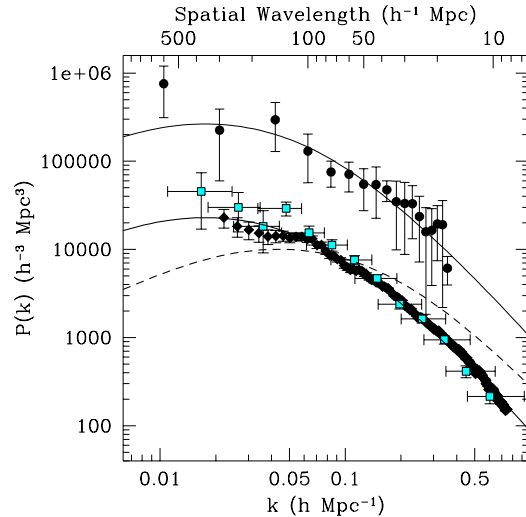


Figure 3. The power spectrum of 2dF galaxies and REFLEX clusters. *Filled diamonds*: estimate using 147,000 redshifts by the 2dF team [19]; *open squares*: Tegmark et al. analysis of the 100,000-redshift public release, with accurate treatment of window aliasing and error covariances [39]; *filled circles*: REFLEX clusters in a  $600 h^{-1} \text{Mpc}$  box [45]. *Dashed line*: Einstein-De Sitter CDM model; *lower solid line*: Lambda-CDM “standard” model (as defined in the first section); both are normalized to match the amplitude of CMB fluctuations [40]; *upper solid line*: same Lambda-CDM model, but renormalized (“biased”) according to the mass selection function of REFLEX clusters [45,13].

spite the great advances of the last few years in our knowledge of the early phases of galaxy formation [38], we are still relatively ignorant about the details of these processes at early epochs. As a consequence  $b$  remains normally a free parameter when comparing galaxy clustering to the models. As I shall discuss shortly, the situation can be more favourable when measuring  $P(k)$  using X-ray selected clusters.

The 2dF and REFLEX surveys have produced the best estimates to date of the power spectrum of galaxies and X-ray clusters, respectively. Fig. 3

compares these data sets directly. One can notice the remarkable similarity of the shape of  $P(k)$  between galaxies and clusters. Such simple proportionality is here seen so clearly thanks to the size and the quality of these two surveys. This provides a direct confirmation of the bias scenario, where clusters form at the high, rare peaks of the mass density distribution [41] and for this reason display a stronger clustering amplitude. In the same figure I have also plotted the predictions for the power spectrum of the mass from two variants of the CDM family, computed as described in [42]. What we defined as the “standard” model in the beginning ( $\Omega_M \simeq 0.3$ ,  $\Omega_\Lambda \simeq 0.7$ ,  $h = 0.7$ ) provides in general an excellent fit to the 2dF power spectrum, with a bias factor (i.e. normalization) close to unity<sup>8</sup>. The upper solid curve, on the other hand, is the same model re-normalized as

$$P_{clus}(k) = b_{eff}^2 P_{CDM}(k) \quad , \quad (1)$$

where the effective bias factor  $b_{eff}$  has been computed taking into account the effective mass range of the cluster sample, using a relatively straightforward theory [43,44] (see [45] for more details). It is for these computations that a well-understood mass selection function of our clustering tracers is crucial. The general result (an additional step with respect to galaxies), is that our fiducial low- $\Omega_M$  CDM model is capable to match very well **both** the shape and amplitude of the cluster  $P(k)$  [45].

This shape agrees well (yet with a different, unknown bias) also with the power spectrum of the distribution of QSO’s from the 2QZ survey, a large redshift survey of colour-selected quasars, also based on the 2dF spectrograph at the Anglo-Australian Telescope [46].

As can be seen from fig. 3, the low- $\Omega_M$  CDM model predicts a maximum for  $P(k)$  around  $k = 0.02 \text{ h Mpc}^{-1}$ . One important meaning of this turnover (which is an imprint of the horizon size

<sup>8</sup>In fact, once we fix the primordial spectrum  $P_o$ , in a pure CDM Universe the observed shape depends only on  $\Omega_M$ , not on  $\Omega_\Lambda$  (which on the other hand influences the normalization). In the literature, this is often parameterized through a *shape parameter*  $\Gamma = \Omega_M h f(\Omega_b)$ , where  $f(\Omega_b) \sim 1$  in case of negligible baryon fraction. Our fiducial “Cosmology 2000” model, therefore, has  $\Gamma \simeq 0.2$ .

at the epoch of matter-radiation equality [5]) is that of an “homogeneity scale”, above which (smaller  $k$ ’s) the variance drops below the Poissonian value. In a pure fractal Universe, for example,  $P(k)$  would continue to rise when moving to smaller and smaller  $k$ ’s [47]. In fact, at least visually the data of Fig. 3 do not really show a convincing indication for a maximum. In addition, on such extremely large scales ( $\lambda > 500 \text{ h}^{-1} \text{ Mpc}$ ), the effect of the survey geometry on the measured power can be very significant, resulting in an effective survey *window function* in Fourier space which is convolved with the true underlying spectrum (e.g. [39]). For highly asymmetric geometries, the plane-wave approximation intrinsic in the Fourier decomposition fails, and the convolution with the window function easily mimics a turnover in a spectrum with whatever shape (e.g [48]). The best solution in such cases is to resort to survey- and clustering-specific eigenfunctions as those provided by the Karhunen-Loeve (KL) transform [49]. An application of this technique to the REFLEX data [50] seems to confirm the reality of a turnover at  $k \simeq 0.023 \text{ h Mpc}^{-1}$ , consistent with a CDM shape parameter  $\Gamma = 0.14^{+0.13}_{-0.07}$ , essentially the same that best describes the current 2dF and CMB data [51], corresponding to an  $\Omega_M \simeq 0.2$  CDM model.

The SDSS will provide unique information around the scale of the expected peak of  $P(k)$ , in particular through the Luminous Red Galaxy (LRG) sample. A first application of the KL transform to very early SDSS angular data is presented in [52], where it is shown that even from only 222 square degrees, the survey is able to sample the peak of the power spectrum. A parallel analysis using a different technique [53] finds a best-fitting CDM spectral shape  $\Gamma = 0.14^{+0.11}_{-0.06}$ , i.e. virtually the same as measured by 2dF and REFLEX, again indicating an impressive convergence of independent observations towards the same low- $\Omega_M$  CDM model.

The SDSS LRG sample will also be useful to verify the presence of *baryonic features*, in  $P(k)$ , due to oscillations in the baryonic component within the last-scattering surface [42]. A possible detection has been claimed in an analysis of some

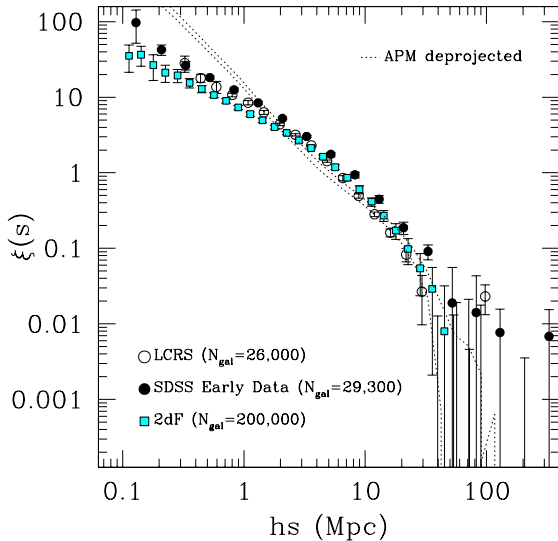


Figure 4. Estimates of the galaxy two-point correlation function from the new 2dF [56] and SDSS [57] data, compared to the previous Las Campanas Redshift Survey [58]. The dotted lines show instead a correlation function in *real space*, obtained through deprojection from the APM 2D galaxy catalogue [59] under two different assumptions about galaxy clustering evolution.

cluster and galaxy samples previous to 2dF and REFLEX [54]. These features are expected to be of very low amplitude<sup>9</sup>, unless the baryon density is much higher than currently established. In fact, similar wiggles seen in the 2dF power spectrum are interpreted as an artifact of the survey window function [19], while the REFLEX data do not show convincing evidence so far.

#### 4.2. The Two-Point Correlation Function

In fact, the simplest statistics one can compute from the data and also that for which the selection function is more directly corrigible, is not the power spectrum, but rather its Fourier transform,

<sup>9</sup>Remember, however, that these considerations are strictly valid for the matter power spectrum, not for the *biased* field represented by galaxies or clusters for which, in principle, one could speculate that such features might be non-linearly amplified.

the *two-point correlation function*  $\xi(r)$ , which measures the excess probability over random to find a galaxy at a separation  $r$  from a given one [55]. Fig. 4 shows the correlation function measured in *redshift space*,  $\xi(s)$  (see next section for definitions), from the 2dF and SDSS current data sets [56,57], compared to the previous LCRS [58]. Also shown (dotted lines) is  $\xi(r)$  reconstructed from the APM angular survey [59].

The figure shows that, especially for the two newest surveys, the shape of  $\xi(s)$  is extremely well described between  $0.1$  and  $50 h^{-1} \text{ Mpc}$ , by a power-law form  $\sim (s/s_o)^{-\gamma}$ , with a *correlation length*  $s_o \simeq 8 h^{-1} \text{ Mpc}$ . The overall difference with the  $\xi(r)$  from the APM survey (which is in real space, being based on a deprojection of angular clustering), is mostly due to redshift-space effects, that I will address in detail in the next section. Note how  $\xi(s)$  maintains a low-amplitude, positive value out to separations of more than  $50 h^{-1} \text{ Mpc}$ , with the 2dF and SDSS data possibly implying a zero-crossing scale approaching  $100 h^{-1} \text{ Mpc}$ . This comparison shows explicitly why large-size galaxy surveys are so important, given the weakness of the clustering signal at these separations<sup>10</sup>.

#### 4.3. Velocity Distortions in the Redshift-Space Pattern

The separation  $s$  between two galaxies computed using their observed redshifts is not a true distance: the red-shift observed in the galaxy spectrum is in fact the quantity  $cz = cz_{\text{cosmological}} + v_{\text{pec||}}$ , where  $v_{\text{pec||}}$  is the component of the galaxy peculiar velocity along the line of sight. This contribution is typically of the order of  $100 \text{ km s}^{-1}$  for galaxies in the general field, but can rise above  $1000 \text{ km s}^{-1}$  within high-density regions as rich clusters of galaxies. Fig. 4 shows explicitly the consequence of such *redshift-space distortion* for the correlation function:  $\xi(s)$  (all points) is *flatter* than its real-space counterpart

<sup>10</sup>There is quite a bit of confusion in technical papers on the term “scale” when comparing results from power spectra and correlation function analyses. A practical “rule of thumb” which works about right with well-behaved spectra is that a scale  $k$  in the power spectrum, corresponding to a spatial wavelength  $\lambda = 2\pi/k$ , relates approximately to  $r \sim \lambda/4$  in  $\xi(r)$ .

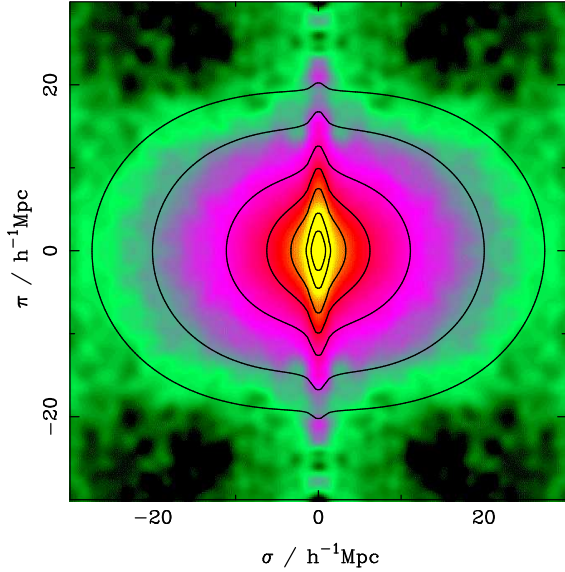


Figure 5. The bi-dimensional correlation function  $\xi(r_p, \pi)$  (with  $r_p$  called instead  $\sigma$ ) from the 2dF redshift survey. The large-scale deviation from circular symmetry is a measure of the level of infall of galaxies onto superclusters, proportional to  $\beta = \Omega^{0.6}/b \simeq 0.43$  [14].

(dotted lines). This is the result of two concurrent effects: on small scales ( $r \lesssim 2 h^{-1} \text{ Mpc}$ ), clustering is suppressed by high velocities in clusters of galaxies, that spread close pairs along the line of sight producing what in redshift maps are sometimes called “Fingers of God”. Some of these are perhaps recognisable in Fig. 1 as thin radial structures. On the other hand, large-scale coherent streaming flows of galaxies towards high-density structures enhance the apparent contrast of these, when seen perpendicularly to the line of sight. This effect, on the contrary, amplifies  $\xi(s)$  above  $\sim 3 - 5 h^{-1} \text{ Mpc}$ , as evident in Fig. 4.

Such peculiar velocity contribution can be disentangled by computing the two-dimensional correlation function  $\xi(r_p, \pi)$ , where the separation vector  $s$  between a pair of galaxies is decomposed into two components,  $\pi$  and  $r_p$ , parallel and perpendicular to the line of sight respectively (see [62] for details). The result is a bidimensional

map, whose iso-correlation contours look as in Fig. 5, where  $\xi(r_p, \pi)$  computed for the 2dF survey is plotted [14].

Redshift-space distortions might seem only an annoying feature, as they hide the true clustering pattern from direct investigation. In fact, they contain important information as galaxy motions are a direct dynamical probe of the mass distribution [63]. Non-linear distortions are a measure of the “temperature” of the galaxy soup on small scales, and they are in principle related to  $\Omega_M$  through a *Cosmic Virial Theorem* [55], which however has been shown to be difficult to apply in practice to real data [64]. Linear distortions produced by infall provide a way to measure the parameter  $\beta = \Omega_M^{0.6}/b$ , i.e. essentially the mass density of the Universe modulo the bias factor. As thoroughly explained in the excellent review by Andrew Hamilton [62], this can be achieved by measuring the oblate compression of the contours of  $\xi(r_p, \pi)$  along  $\pi$ . One way to do this is to expand  $\xi(r_p, \pi)$  in spherical harmonics. In linear perturbation theory, only the monopole  $\xi_0(s)$ , quadrupole  $\xi_2(s)$  and hexadecapole  $\xi_4(s)$  are non-zero, and  $\beta$  can in principle be derived directly through the following ratio, which should be independent of  $s$  [62]

$$\frac{\xi_2(s)}{\xi_0(s) - \bar{\xi}_0(s)} = \frac{\frac{4}{3}\beta + \frac{4}{7}\beta^2}{1 + \frac{2}{3}\beta + \frac{1}{5}\beta^2}, \quad (2)$$

where  $\bar{\xi}_0(s) = 3s^{-3} \int_0^s \xi_0(x)x^2 dx$  is the averaged correlation function within the radius  $s$ . In practice, linear and non-linear effects are interlaced out to fairly large scales ( $\sim 20 h^{-1} \text{ Mpc}$ ), and require a careful modeling. This has been done, using a simple but effective phenomenological approach, for the 2dF correlation function of Fig. 5, producing one of the most remarkable results of past year [14]; the 2dF quadrupole-to-monopole ratio is best reproduced<sup>11</sup> by a model with  $\beta = 0.43 \pm 0.07$ . If 2dF galaxies are unbiased ( $b \simeq 1$ ), this would imply  $\Omega_M \simeq 0.25$ .

Clusters of galaxies clearly also partake in the overall motion of masses produced by cosmolog-

<sup>11</sup>Since the conference, a more sophisticated error analysis was applied to the 100,000 redshift public release [39], obtaining essentially the same value of  $\beta$ , but with a 1- $\sigma$  error of  $\pm 0.16$ .

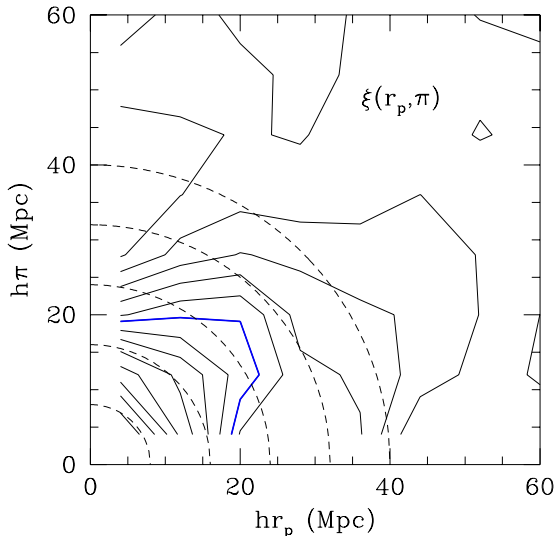


Figure 6.  $\xi(r_p, \pi)$  from the REFLEX survey of X-ray clusters of galaxies (here limited to the first quadrant only, where all the information is contained). Note the compression of the contours along the redshift ( $\pi$ ) direction, evidence of significant streaming velocities towards high-density regions, and the lack of any stretching at very small  $r_p$ 's (there are no “Fingers of God” made by clusters!) [60,61].

ical inhomogeneities. Line-of-sight spurious effects (as projections in optically-selected cluster catalogues [65] or large redshift errors) and limited statistics, prevented so far the detection of true velocity anisotropies in cluster  $\xi(r_p, \pi)$  maps. Fig. 6 plots  $\xi(r_p, \pi)$  for the REFLEX survey. Here we have a clear indication of compression of the contours along the line of sight, of the kind expected by the linear infall of clusters towards superstructures. The statistical signature of cluster motions seems therefore to have been detected, and at the time of writing accurate experiments using large mock realisations of the REFLEX survey are under way, to quantify precisely the confidence level at which  $\beta$  can be estimated from this map [60,61].

## 5. STRUCTURE AT HIGH REDSHIFTS AND GALAXY FORMATION

The final part of my talk was dedicated to a quick overview of the status of large-scale structure studies at  $z \gtrsim 1$  and its intimate connection with the formation of galaxies themselves. It is practically impossible with the limited space available here to give a fair account of the fervent activity in the field of galaxy formation and evolution. For this, the reader is addressed to other more specific reviews available in the literature (e.g. the excellent lectures by Ellis in [38]). Here I will limit the discussion to some specific points concerning the possibility to trace the evolution of structure back in time using galaxy redshift surveys.

### 5.1. Evolution of Clustering

Ideally, studying the evolution of structure through deep ( $z > 0.5$ ) redshift surveys would provide a further powerful way to constrain models and in particular to measure cosmological parameters as  $\Omega_M$ , which governs the growth rate of structures. This ideal dream is in practice hampered by two factors. First, in a classical magnitude-limited survey the *k-correction*<sup>12</sup> depends on the spectral type, thus making the relative percentage of morphological types be a function of redshift. For example, when observing in a blue band the *k-correction* for elliptical galaxies (which have a red spectrum) grows much more rapidly than for young blue galaxies as spirals or irregulars. Since we know that locally red galaxies are more clustered than blue galaxies (e.g. [57], just because of this effect one would measure a fainter clustering at high  $z$ , independent of the growth rate of structure. Secondly, and additionally, galaxies do evolve and at large redshifts even a population selected, e.g., with the same rest-frame colour and luminosity range as locally (i.e. properly *k-corrected*) would include galaxies which are very probably not the progenitors of a local survey like 2dF and SDSS. Also in this case, we would not be looking at the same tracers

<sup>12</sup>That is, the fraction of light lost because of the red-shifting and stretching of the spectrum at larger and larger distances

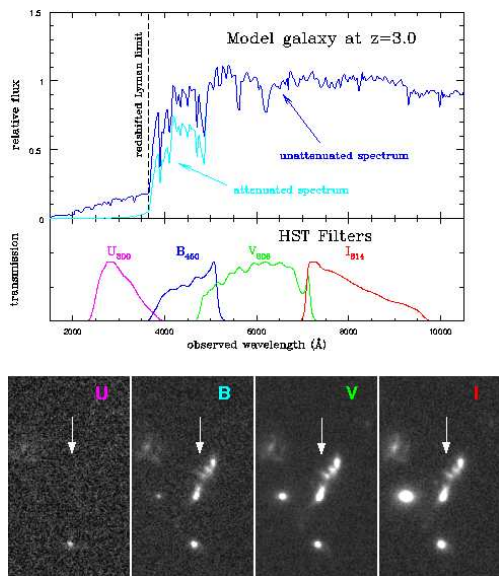


Figure 7. How to select “a priori” candidate galaxies at  $z = 3$ : in this figure by Marc Dickinson [71], the band-dropout technique is pedagogically outlined. The upper panel shows the spectrum of a star-forming galaxy at  $z = 3$ , and the wavelength position of four filters covering the UV-visible range. The corresponding galaxy images in the four bands are displayed in the bottom CCD frames, with the object disappearing in the U band due to the almost complete absorption below the redshifted Lyman limit.

at different redshifts, and so the observed evolution of the correlation function or power spectrum would be impossible to connect to the growth rate of fluctuations. This introduces a profound difference with “local” surveys, where the look-back time is small compared to Hubble time: deep galaxy redshift surveys trace at the same time the growth of the mass skeleton of the Universe and the formation and evolution of the stellar population in the galaxies themselves.

These difficulties are reflected by the lack of a consistent trend in the evolution of the correlation length measured from available deep surveys, that show values scattered between 1.8 and  $5 h^{-1} \text{Mpc}$  for redshifts in the range  $[0,1]$  (see

Table 1 in [66] for a review). The large variance among different samples reflects the problems outlined above, as the use of different spectral bands (e.g. red-selected or blue-selected surveys), exacerbated by the limited size of surveyed areas ( $\sim 100 \text{ arcmin}$ ), due to the time needed to collect a spectrum for  $z \simeq 1$  galaxies. It is probably for these reasons that most progress in the area of the evolution of clustering has come during the last few years from 2D surveys, measuring angular clustering over fairly large angles thanks to wide-angle CCD cameras (see e.g. [67] and references therein).

This situation is therefore yet another example in the long list of “cosmological probes” which rather than cosmology turned out to be testing evolution of a particular class of objects (were they either radio galaxies, first-ranked cluster galaxies, or generic galaxies). This shifts the attention in deep surveys from just using galaxies as “test particles” to understanding the way their baryonic component was assembled and evolved as to shape today’s colours and morphologies [38,66]. There are therefore good reasons for going deeper with redshift surveys: the picture becomes probably more complicated to interpret cosmologically, but certainly richer in astrophysical details. “Big” questions that need investigation at high  $z$  are, for example, (1) do we see evidence of continuous merging, as expected in the “standard” hierarchical model? (2) Can we reconcile with this scenario the observation of a consistent fraction of old massive elliptical galaxies at  $z > 1$ ? (3) How the assembly of galaxy masses translates into the star formation history of the Universe? (4) How do we connect this to the ionization history of the Universe? (5) How did galaxy morphologies (and their relation with local density) originate? [38]

## 5.2. Clustering at $z > 1$ : High-bias Objects

The best current flux-limited deep surveys reach  $z \sim 1$  [68,69]. However, if the goal is to select samples at very large redshift, moving the flux (magnitude) limit to even fainter values is not the most efficient option (although it guarantees a higher level of control over selection effects). Alternatively, an important advance of the last few

years has been the ability to select through photometric means (i.e. using CCD images in different filters), almost volume-limited samples of galaxies with mean redshifts  $z \simeq 3$  and  $\simeq 4$  [66,70]. This is an efficient alternative to pure flux-limited samples, which even at very faint magnitude limits are dominated by a bulk of faint  $z < 0.5$  objects. The technique is based on the detection of specific features (“breaks”) in galaxy spectra using multi-band imaging through appropriate sets of filters. The most notable of such features is the Lyman break at 912 Å which is prominent in star-forming galaxies. At  $z = 3$ , the break is redshifted to 3650 Å, thus falling between the so-called  $U$  and  $B$  filters. For this reason, a star-forming  $z \sim 3$  galaxy will be detected in  $B$ , but will be almost invisible in  $U$  (see Fig. 7). A similar reasoning can be applied to hunt for  $z \sim 4$  galaxies, using instead the  $B$  and  $V$  filters. A fairly large sample ( $\sim 1000$  galaxies) at  $z = 3$  has been constructed in this way during the 1990’s by Steidel and collaborators, spectroscopically confirmed through intense use of the Keck 10-m telescopes [70].

Ly-break galaxies turn out to be *highly biased* objects. In fact, they show a very strong clustering, with a correlation length comparable to that of normal galaxies at the present epoch [72]. This implies that they cannot be representative of the mass clustering at that epoch. A consistent explanation is that they are the progenitors of massive elliptical galaxies that today populate rich clusters of galaxies, undergoing their most active phase of star formation [73].

### 5.3. Future Deep Redshift Surveys

Although custom-selected samples of high-redshift objects as Lyman-break galaxies are certainly fundamental for understanding specific scientific issues, it is difficult to use them to trace the evolution of the overall population. To make a further major step in our understanding of how structure and galaxies formed and evolved, we need new surveys which: (1) Are based on multi-band photometric information, such that selection effects can be understood as finely as possible and specific morphologies and rest-frame colours can be traced back in time over a sensible range;

(2) Cover areas which are wide enough to reduce “cosmic variance”; (3) Provide, a combination of depth, volume and statistics (number of objects) comparable to local ongoing surveys as 2dF and SDSS.

There are currently two ambitious projects which are due to start during 2002 and that are expected to be close to these *desiderata*. One is the DEEP2 survey [74], that will collect spectra for  $\sim 60,000$  galaxies between  $z \sim 0.7 - 1.5$ , over four  $2^\circ$  by  $0.5^\circ$  strips of sky using the Keck 10 m telescope. The other is the VIRMOS survey, that will similarly observe  $\sim 150,000$  galaxy spectra using mainly the new VIMOS spectrograph at the VLT 8 m telescope, splitted into a “wide” survey over  $\sim 16 \text{ deg}^2$  to a red magnitude  $I_{AB} = 22.5$  ( $\sim 100,000$  redshifts), plus a “deep” survey over  $\sim 1 \text{ deg}^2$  to  $I_{AB} = 24$  ( $\sim 50,000$  redshifts), in addition to one or more “ultra-deep” probes to  $I_{AB} = 25$  over some arcminute-sided fields, using an Integral Field Unit [75].

## 6. SUMMARY

In conclusion, I hope to have passed the sensation that we do live in a glorious time for cosmology, which has finally become a mature science, not anymore an entertaining playground for almost pure speculation. In fact, we never had such a wealth of data at our disposal, by which we are pinning down the values of cosmological parameters to high accuracy (e.g. [2]), while at the same time being able to study galaxy formation almost in the act, thanks to new powerful telescopes. The few observational facts we have reviewed here contribute to further reinforce the remarkable convergence of different observables (CMB, large-scale structure, distant Supernovae, cluster evolution, to mention a few) towards what we called in the introduction the current standard model, i.e. one with a flat geometry ( $\Omega_{total} = 1$ ), apparently guaranteed by the combination of a dominating Cold Dark Matter component ( $\Omega_{CDM} \simeq 0.3$ ,  $\Omega_{baryon} \simeq 0.02$ ) and a Dark Energy of unknown nature (the cosmological constant,  $\Omega_\Lambda \simeq 0.7$ ). Several interesting talks at the TAUP2001 meeting were devoted to the detection of baryonic and non-baryonic dark

matter. I invite the reader to look at the corresponding contributions in this volume, however, and test whether he/she is not left with some uneasiness as our wonderful “standard” cosmological model seems in fact to be so far essentially based on a) a *Dark Matter* we do not detect; b) a *Dark Energy* we do not understand; c) a fraction of Baryons we cannot completely find! Yet everything seems to work: isn’t this reminiscent of epicycles?

**Acknowledgments.** I thank the organizers of TAUP2001 for inviting me to give this review, and in particular Alessandra Di Chiarico for her patience in waiting for this contribution. I am grateful to all my collaborators without whom many of the results discussed here would not be reality, in particular P. Schuecker, C. Collins and H. Böhringer, and to A. Fernandez-Soto for a careful reading of the manuscript and useful discussions. I thank I. Zehavi and E. Hawkins for providing their clustering results in electronic form.

## REFERENCES

1. Blumenthal, G.R., 1984, *Nature*, 311, 517
2. De Bernardis, P., et al., 2000, *Nature* 404, 955
3. Perlmutter, S., Riess, A., 1999, in “COSMO-98: II Int. Workshop on Particle Physics and the Early Universe”, D.O. Caldwell ed., AIP Conference Proceedings, vol. 478., (Woodbury, NY), p. 129
4. Peacock, J.A., 1999, *Cosmological Physics* (Cambridge: Cambridge University Press)
5. Padmanabhan, T., 1993, *Structure Formation in the Universe* (Cambridge: Cambridge University Press)
6. White, S.D.M., & Rees, M.J., 1978, *MNRAS*, 183, 341
7. Jenkins, A., et al., 2001, *MNRAS*, 321, 372
8. Somerville, R.S., 2001, *MNRAS*, 320, 504
9. Kauffmann, G., Charlot, S., Haehnelt, M., 2000, *Phil. Trans. of the Royal Soc. of London, Series A*, Vol. 358, p. 2121
10. Cole, S., et al., 2000, *MNRAS*, 319, 168
11. Silva, L., et al., 2001, *Ap&SS*, 276, 1073
12. Maddox, S.J., et al., 1990, *MNRAS*, 242, 43p
13. Borgani S., Guzzo L., 2001, *Nature* 409, 39
14. Peacock, J.A., et al. (the 2dF Team), 2001, *Nature* 410, 169
15. Rood, H.J., 1998, *ARA&A*, 26, 245
16. Colless, M., et al. (the 2dFGRS team), 2001, *MNRAS*, 328, 1039
17. Shectman, S.A., et al., 1996, *ApJ*, 470, 172
18. Vettolani, G., et al. (the ESP team), 1998, *A&AS*, 130, 323
19. Percival, W., et al. (the 2dFGRS team), 2001, *MNRAS* 327, 1297
20. Norberg, P., et al. (the 2dFGRS team), 2001, *MNRAS*, 328, 64
21. Peacock, J.A. & the 2dFGRS team, 2002, in *20th Texas Symposium on Relativistic Astrophysics*, (Austin, December 2000), in press (astro-ph/0105450)
22. York, D.G., et al. (the SDSS Collaboration), 2000, *AJ*, 120, 1579
23. Fernández-Soto, 2001, A., *Ap&SS*, 276, 965
24. Yee, H., 1998, in *Xth Rencontres de Blois: The Birth of Galaxies*, in press (astro-ph/9809347)
25. Becker, R.H. & the SDSS Collaboration, *AJ* (2002), in press (astro-ph/0108097)
26. Eisenstein, D.J., et al. (the SDSS Collaboration), 2001, *AJ*, 122, 2267
27. Guzzo, L., 2000, in *XIXth Texas Symposium on Relativistic Astrophysics & Cosmology*, Nucl. Phys. B (Proc. Suppl.) vol.80, p.233 (09/06), E. Aubourg et al. eds. (astro-ph/9911115)
28. Nichol, R.C., 2002, in *Tracing Cosmic Evolution with Galaxy Clusters*, ASP Conf. Series, S. Borgani et al. eds., in press (astro-ph/0110231)
29. Bartlett, J.G., 2002, in *Tracing Cosmic Evolution with Galaxy Clusters*, ASP Conf. Series, S. Borgani et al. eds., in press (astro-ph/0111211)
30. Ellis, R.S., 2002, in *Tracing Cosmic Evolution with Galaxy Clusters*, ASP Conf. Series, S. Borgani et al. eds., in press (astro-ph/0112540)
31. Borgani, S., et al., 2001, *ApJ*, 561, 13
32. Rosati, P., et al., 1995, *ApJ* 445, L11
33. Böhringer, H., et al. (the REFLEX Team), 2001, *A&A* 369, 826
34. Henry, J.P., 2002, in “AMiBA 2001: High-z Clusters, Missing Baryons, and CMB Polarization”, in press (astro-ph/0109498)
35. Rosati, P., Borgani, S., & Norman, C., 2002, *ARAA*, in preparation
36. Yair, S., Branchini, E., Dekel, A., 2000, *ApJ* 540, 62
37. Benoist, C., et al., 1999, *ApJ* 514, 563
38. Ellis, R., 2001, in “Lectures of the XIth Canary Island Winter School of Astrophysics” (astro-ph/0102056)
39. Tegmark, M., Hamilton, A.J.S., Xu, Y., 2002, *MNRAS*, submitted (astro-ph/0111575)

40. Bunn, E.F., & White, M., 1997, ApJ, 480, 6
41. Kaiser, N., 1984, ApJ 284, L9
42. Eisenstein, D.J., Hu, P., 1998, ApJ 496, 605
43. Mo, H.J., & White S.D.M., 1996, MNRAS 282, 347
44. Sheth, R.K., Mo, H.J., Tormen, G., 2001, MNRAS 323, 1
45. Schuecker, P., et al. (the REFLEX Team), 2001, A&A 368, 86
46. Hoyle, F., et al., 2002, MNRAS, 329, 336
47. Guzzo, L., 1997, New Astronomy, 2, 517
48. Carretti, E., et al., 2001, MNRAS, 324, 1029
49. Vogeley, M.S., Szalay, A.S., 1996, ApJ 465, 34
50. Schuecker, P., et al. (the REFLEX Team), 2002, in preparation
51. Efstathiou, G.P., et al. (the 2dFGRS team), 2002 MNRAS, in press (astro-ph/0109152)
52. Szalay, A.S., et al. (the SDSS Collaboration), 2001, ApJ, submitted (astro-ph/0107419)
53. Dodelson, S., et al. (the SDSS Collaboration), 2001, ApJ, submitted (astro-ph/0107421)
54. Miller, C.J., Nichol, R.C., Batuski, D.J., 2001, ApJ 555, 68
55. Peebles, P.J.E., 1980, *The Large-Scale Structure of the Universe*, (Princeton: Princeton University Press)
56. Hawkins, E., et al. (the 2dFGRS team), 2002, in preparation
57. Zehavi, I., et al. (the SDSS Collaboration), 2002, ApJ, 571, in press (astro-ph/0106476)
58. Tucker, D.L., et al., 1997, MNRAS, 285, L5
59. Baugh, C.M., 1996, MNRAS, 280, 267
60. Collins, C.A., et al. (the REFLEX Team), 2000, MNRAS 319, 939
61. Guzzo, L. et al. (the REFLEX Team), 2002, in preparation
62. Hamilton, A.J.S., 1998, in *The Evolving Universe. Selected Topics on Large-Scale Structure and on the Properties of Galaxies*, (Dordrecht: Kluwer), ASSL Series, vol. 231, p. 185 (also, astro-ph/9708102).
63. Kaiser, N., 1987, MNRAS, 227, 1
64. Fisher, K.B., et al., 1994, MNRAS, 267, 927
65. Collins, C.A., et al., 1995, MNRAS, 274, 1071
66. Steidel, C., 1999, in *Evolution of large scale structure: from recombination to Garching*, A. J. Banday et al. eds., (Garching: European Southern Observatory), p.380
67. McCracken, H., et al., 2002, A&A, in press (astro-ph/0107526)
68. Le Fevre, O., et al., 1996, ApJ, 461, 534L
69. Carlberg, R.G., 2001, ApJ, 563, 736
70. Steidel, C.C., & Hamilton, D., 1992, AJ, 104, 941
71. Dickinson, M., 1998, in *The Hubble Deep Field*, STScI Symposium, M. Livio et al. eds., (New York : Cambridge University Press), p.219
72. Giavalisco, M., et al., 1998, ApJ 503, 543
73. Governato, F., et al., 1998, *Nature*, 392, 359
74. Coil, A.L., 2001, PASP, 113, 1312
75. O. Le Fèvre, et al. (the VIRMOS Consortium), 2001, in *Deep Fields*, S. Cristiani et al. eds., Berlin: Springer, p. 236